Flexible Coordination Polymers

Porous Coordination-Polymer Crystals with Gated Channels Specific for Supercritical Gases**

*Ryo Kitaura, Kenji Seki, George Akiyama, and Susumu Kitagawa**

Considerable effort has been devoted to the synthesis and characterization of new crystalline nanosized porous materials, such as coordination polymers and inorganic zeolites, because of their versatile applicability to gas storage, molecular sieves, size- or shape-selective catalysis, and ion exchange.[1–7] For successful performance of these functions, robustness and stability of the porous frameworks are essential. In contrast, flexible host frameworks that respond to guest molecules, for example, induced-fit recognition between a protein and its substrate, have high selectivity for guest inclusion. Coordination polymers, in spite of their crystalline form, are suitable for creating flexible and dynamic porous frameworks, so-called third-generation compounds,[8] because the wide variety of architectures and topologies are based not only on coordinative bonds, but also on hydrogen bonds and/or π–π stacking, which are weaker than the Si–O and Al–O bonds in zeolites.[9–13] Hence, we focused on the preparation of two new types of flexible and dynamic nanoporous frameworks created by coordination polymers with interdigitation and interpenetration, and examined the gas-adsorption properties (CO_2, CH_4, O_2, and N_2) at high pressure and ambient temperature.

Our strategy for functional coordination polymers that respond to guest molecules is to assemble rigid motifs with a degree of freedom in displacement to provide two types of integrated frameworks (Figure 1): framework A with mutually interdigitated two-dimensional (2D) motifs, and framework B with mutually interpenetrated three-dimensional (3D) motifs. Both the rigidity of a structural motif and a degree of freedom in displacement could give rise to flexibility of the whole framework and thus improve porous properties. A coordination polymer of type A, namely, $[Cu(dhbc)_2(4,4'\text{-bpy})]\cdot H_2O$ (**1a**), was prepared from Cu^{II} nitrate, 2,5-dihydroxybenzoic acid (Hdhbc), and 4,4′-bipyridine (4,4′-bpy). The copper ions are connected by 4,4′-bpy to produce straight chains, and linked by dhbc to give a 2D sheet motif (Figure 2a and b, respectively). The motif has interlocking ridges and hollows constructed by the dhbc benzene planes in an upright fashion. The distance of 3.443 Å between the planes of the nearest-neighbor dhbc ligands indicates the presence of π–π stacking interactions, and the motifs are mutually interdigitated to create 1D channels along the *a* axis with a cross section of 3.6 × 4.2 Å (Figure 2c), in which one water molecule is included per copper ion. The type B coordination polymer **2** was obtained by using Cu^{II}, benzene-1,4-dicarboxylate (bdc), and 4,4′-bpy. Two-dimensional grid-type sheets composed of Cu^{II} and bdc are linked by 4,4′-bpy to produce a 3D jungle-gym-like framework, similar to the structure of Prussian Blue. Two independent 3D structures interpenetrate each other to form a 3D framework with cylindrical channels with approximate dimensions of 3.4 × 3.4 Å along the *c* axis (Figure 3).[14]

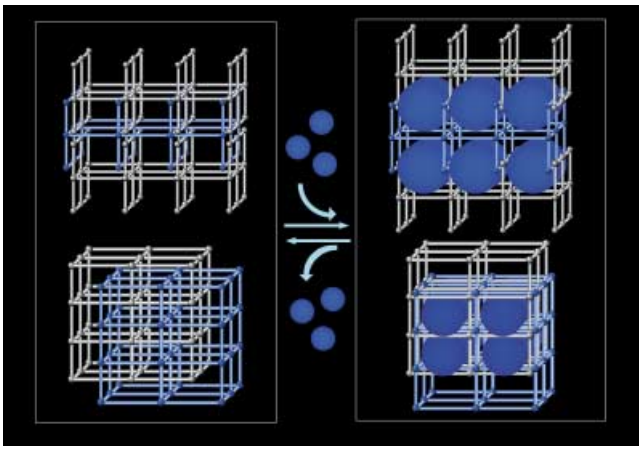

Figure 1. Schematic representation of dynamic frameworks. Above: Interdigitated framework of layers whose gap depends on the guest molecules. Below: Interpenetrated framework whose interunit space depends on the guest molecules.

Thermogravimetric analysis of **1a** shows the release of water molecules of crystallization with increasing temperature up to 120 °C to give guest-free anhydrous **1b**. No further weight loss was observed between 120 °C and 170 °C, that is, the guest-free phase is stable. Since the X-ray powder diffraction (XRPD) pattern of **1b** (Figure 4) shows sharp diffraction peaks similar to those of **1a**, the porous framework is largely maintained, even without water molecules. Detailed comparison of the two XRPD patterns reveals that only small shifts were observed for the peaks (010) and (100), which are attributed to the *ac* and *bc* planes, respectively. Therefore, the 2D layer motif is retained during dehydration. On the other hand, peaks corresponding to the relative position of the layer motifs show an apparent shift to the higher angle region between 15 and 20°. This result clearly indicates shrinking of the layer gap along the *c* axis, which is attributable to a gliding motion of the two π-stacked rings, which decreases the channel cross section.

[*] Prof. Dr. S. Kitagawa, R. Kitaura, G. Akiyama
Department of Synthetic Chemistry and Biological Chemistry
Graduate School of Engineering
Kyoto University
Yoshida, Sakyo-ku, Kyoto 606-8501 (Japan)
Fax: (+81) 75-753-4979
E-mail: kitagawa@sbchem.kyoto-u.ac.jp
K. Seki
Energy Conversion and Storage Technology
Applied Research Centre
Research and Development Department
Osaka Gas Co., Ltd.
6-19-9, Torishima, Konohana-ku, Osaka 554-0051 (Japan)

[**] This work was supported by Grant-in-Aid for Creative Scientific Research (No. 13GS0024), Ministry of Education, Culture, Sports, Science, and Technology, Japan.

Supporting information for this article is available on the WWW under http://www.angewandte.org or from the author.

  0044-8249/03/11504-0444 $ 20.00+.50/0

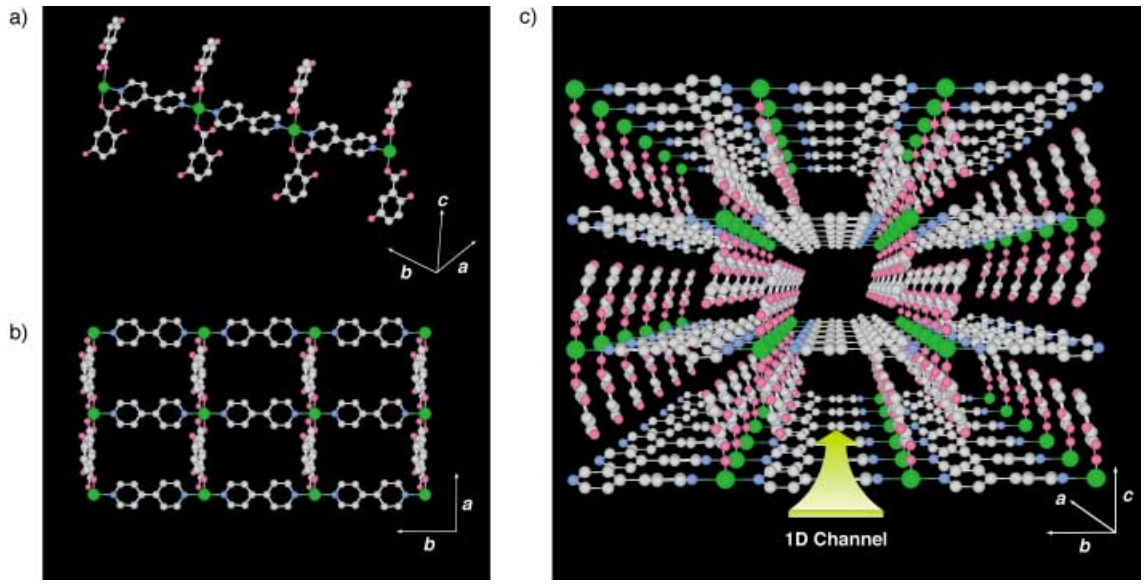

Figure 2. Crystal structure of **1a**. a) 1D chain structure constructed by Cu^{II}, 4,4′-bpy, and dhbc along the *b* axis (Cu, green; O, red; C, gray; N, blue). b) 2D layer structure along the *ab* plane. c) 3D π-stacked pillared layer structure of **1a**. Hydrogen atoms and water molecules are omitted for clarity.

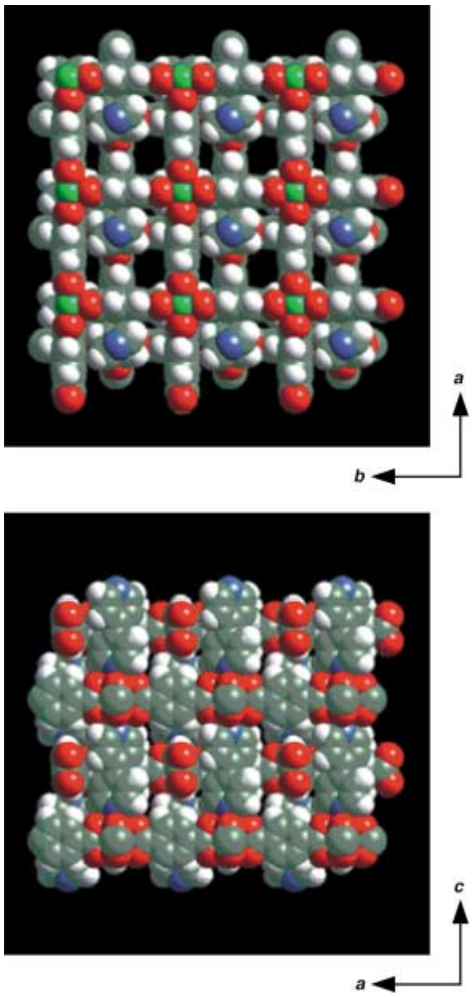

Figure 3. Space-filling model of the crystal structure of **2**. The structure model was optimized by molecular mechanics (MM) with the program package Cerius2.

Compound **1b** shows a type II nitrogen adsorption isotherm at 77 K, and the calculated BET specific surface area is 24 $m^2 g^{-1}$ (see Supporting Information). This low specific surface area leads to the conclusion that nitrogen molecules (molecular size 3.3 Å) could not diffuse into the micropores at all. If the original cross section of **1a** were retained, the nitrogen molecules would readily diffuse into the channels. This also indicates pore contraction on dehydration, as was demonstrated by XRPD. Figure 5a shows the N_2 adsorption isotherm of **1b** in the pressure range between 1 and 120 atm at 298 K. Unlike the adsorption profile at 77 K, the isotherm shows a profile unlike the usual adsorption patterns—a flat curve indicative of no adsorption in the lower pressure region, with an abrupt increase at a pressure of 50 atm (point a), as if channels large enough for the molecule already existed. Langmuir plots are almost linear in the higher pressure region and give a specific surface area of 320 $m^2 g^{-1}$. This high specific surface area clearly shows that nonporous phase **1b** was transformed into microporous phase **1a**. This onset pressure at which the channels of **1b** change into open gates is referred to as the gate-opening pressure.[15] Interestingly, the desorption isotherm shows an abrupt decrease at 30 atm (gate-closing pressure, point b), indicative of hysteresis in the adsorption and desorption isotherms. This hysteretic profile could be repeated many times. This hysteretic sorption behavior is well reproduced by the sum of the isotherms for nonporous phase **1b** and porous phase **1a**. Red and blue dashed lines in Figure 5a represent the estimated adsorption isotherms for nonporous phase and microporous phase, respectively. Below the gate-opening pressure, the adsorption isotherm coincides with the red line for the nonporous phase. Above the gate-opening pressure, the adsorption isotherm starts to approach the blue line (porous phase), and they coincide above 100 atm. At the gate-opening pressure, nitrogen molecules result in transformation

  0044-8249/03/11504-0445 $ 20.00+.50/0

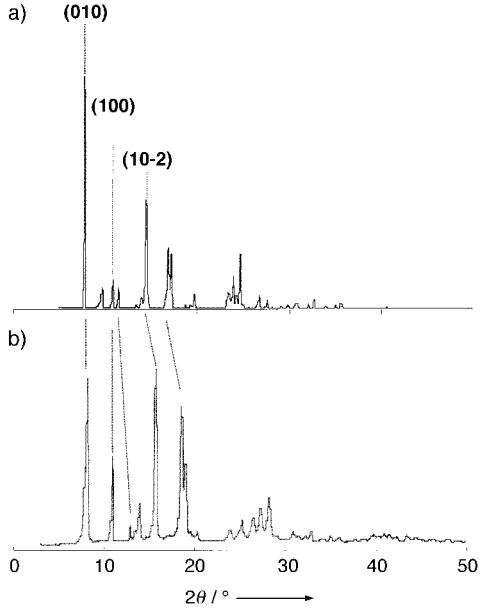

Figure 4. a) Observed XRPD pattern for the as-synthesized sample of **1a**. b) XRPD pattern for the anhydrous sample **1b** (dried at 110 °C under reduced pressure for 5 h). Estimated channel size based on the peak shift of (10−2) is 3.0×3.6 Å.

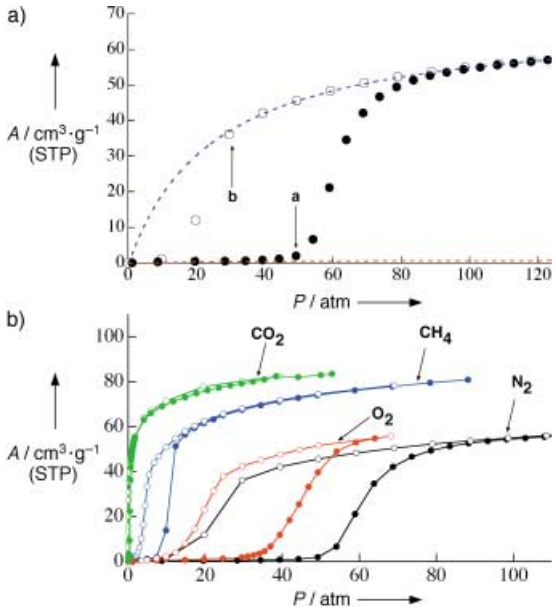

Figure 5. a) Nitrogen adsorption (filled circles) and desorption isotherms (open circles) for **1b** at 298 K. Blue and red dashed lines were determined by fitting the linear parts of the Langmuir plots in the higher (from 83 to 122 atm) and lower (from 8 to 34 atm) pressure ranges, respectively. b) Adsorption (filled circles) and desorption (open circles) isotherms of N_2, CH_4, CO_2 and O_2 at 298 K.

of crystalline "closed" form **1b** into crystalline "open" form **1a**.[15,16] Once nitrogen gas is adsorbed into the micropores of **1a**, nitrogen molecules stabilize the porous phase. Therefore, in the desorption isotherm, the porous phase was maintained until the pressure reached 30 atm (gate-closing pressure). This crystal structure transformation triggered by guest molecules was confirmed by an XRPD measurement on **1b** containing adsorbed methanol (molecular size 4.2 Å; see Supporting Information). To the best of our knowledge, this is the first example of hysteretic sorption behavior of supercritical nitrogen gas at ambient temperature under high pressure. Structural transformation triggered by a supercritical gas, which only exhibits weak dispersive interactions in this system, is facilitated by the unusual framework flexibility provided by displacement of π–π stacked moieties. Figure 5b shows the adsorption isotherms for various gases on **1b** in the pressure range between 1 and 100 atm at 298 K. All of the isotherm profiles are essentially similar to that for N_2 at 298 K, but a clear difference is observed for the gate-opening and gate-closing pressures. The gate-opening pressures for nitrogen, oxygen, and carbon dioxide are 50, 35, and 0.4 atm, and the gate-closing pressures 30, 25, and 0.2 atm, respectively. This difference should be attributable to differences in the intermolecular interaction force of the guest molecules. Similar adsorption behavior was observed for **2** (see Supporting Information).

Many coordination polymers have been synthesized with the aim of achieving stable microporous structures like those of zeolites; however, the goal here is not to mimic zeolites but to create new properties characteristic of coordination polymers. A coordination polymer is the best candidate for realizing of the unique nanostructure reported here. Guests are permitted to pass the gate at a specific gate-opening pressure that depends on the strength of the intermolecular interaction. We expect that such coordination polymers will find applications in gas separation, sensors, switches, and actuators. This flexible and dynamic coordination network opens up a new field in porous coordination materials.

Experimental Section

Synthesis of **1a**: A diethyl ether solution (20 mL) containing a mixture of 4,4′-bpy (0.13 g, 0.8 mmol) and Hdhbc (0.50 g 3.2 mmol) was carefully layered on the top of an aqueous solution (20 mL) of $Cu(NO_3)_2{\cdot}3H_2O$. Platelike green crystals began to form over a few days. One of these crystals was used for X-ray crystallography. The green crystals were collected by filtration, washed with ethanol, and dried under reduced pressure for 2 h. Yield: 0.18 g (0.32 mmol, 41 %). Elemental analysis (%) calcd for $C_{24}H_{14}N_2O_{10}Cu$: C 54.81, H 3.45, N 5.33; found: C 54.64, H 4.04, N 5.12. IR (KBr pellet): $\tilde{\nu}$ = 2810m, 1613s, 1492s, 1383w, 1279w, 1241m, 1131w, 1073w, 820s, 785s, 688m, 648w 554w and 493m cm^{-1}.

Single-crystal X-ray structure determination on **1a**: intensities were measured at 298 K with a graphite-monochromatized $Mo_{K\alpha}$ radiation source (λ = 0.71069 Å). 2198 independent reflections (8955 total measured) were analyzed by a direct method using the SIR92 program and expanded by Fourier techniques. Hydrogen atoms of hydroxy groups were located in the Fourier difference map. Hydrogen atoms except for those of hydroxy groups were placed in idealized positions, and their parameters were not refined. Crystal data: $C_{24}H_{22}CuN_2O_{10}$, M_r = 561.99, monoclinic, space group *P*2/*c* (No. 13), a = 8.167(4), b = 11.094(8), c = 15.863(2) Å, β = 99.703(4)°, V = 1416(1) Å^3, Z = 2, R = 0.068, wR = 0.088. CCDC-191853 contains the supplementary crystallographic data for this paper. These data can be obtained free of charge via www.ccdc.cam.ac.uk/conts/retrieving.html (or from the Cambridge Crystallographic Data Centre, 12, Union Road, Cambridge CB21EZ, UK; fax: (+44) 1223-336-033; or deposit@ccdc.cam.ac.uk).

  0044-8249/03/11504-0446 $ 20.00+.50/0

Coordination polymer **2** was synthesized according to a published procedure. Elemental analysis (%) calcd for $C_{13}H_8NO_4Cu$: C 51.06, H 2.62, N 4.58; found C 50.62, H 2.45, N 4.60.

Gas adsorption measurements: Sorption isotherms were measured at 298 K on an FMS-BG (BEL inc.) automatic gravimetric adsorption measurement system with Rubotherm magnet coupling balance incorporated in a SUS steel pressure chamber. A known weight (200–300 mg) of the as-synthesized sample was placed in the aluminum sample cell in the chamber, and the sample was dried under high vacuum at 373 K for 5 h to remove the host water molecules. The adsorbate was dosed into the chamber, and the change in weight was monitored. After correction for buoyancy, the absorbed amount was determined.

Received: August 27, 2002 [Z50052]

[1] G. A. Ozin, A. Kuperman, A. Stein, *Angew. Chem.* **1989**, *101*, 373–390; *Angew. Chem. Int. Ed. Engl.* **1989**, *28*, 359–376.
[2] A. Corma, *Chem. Rev.* **1997**, *97*, 2373–2419.
[3] M. Eddaoudi, D. B. Moler, H. Li, B. Chen, T. M. Reineke, M. O'Keeffe, O. M. Yaghi, *Acc. Chem. Res.* **2001**, *34*, 319–330.
[4] M. Eddaoudi, J. Kim, N. Rosi, D. Vodak, J. Wachter, M. O'Keeffe, O. M. Yaghi, *Science* **2002**, *295*, 469–472.
[5] B. Moulton, M. J. Zaworotko, *Chem. Rev.* **2001**, *101*, 1629–1658.
[6] J. S. Seo, D. Whang, H. Lee, S. I. Jun, J. Oh, Y. J. Jeon, K. Kim, *Nature* **2000**, *404*, 982.
[7] S. Noro, S. Kitagawa, M. Kondo, K. Seki, *Angew. Chem.* **2000**, *112*, 2162–2164; *Angew. Chem. Int. Ed.* **2000**, *39*, 2082–2084.
[8] S. Kitagawa, M. Kondo, *Bull. Chem. Soc. Jpn.* **1998**, *71*, 1739–1753.
[9] R. Robson, *J. Chem. Soc. Dalton Trans.* **2000**, *21*, 3735–3744.
[10] A. J. Fletcher, E. J. Cussen, T. J. Prior, M. J. Rosseinsky, C. J. Kepert, K. M. Thomas, *J. Am. Chem. Soc.* **2001**, *123*, 10001–10011.
[11] D. V. Soldatov, J. A. Ripmeester, S. I. Shergina, I. E. Sokolov, A. S. Zanina, S. A. Gromilov, Y. A. Dyadin, *J. Am. Chem. Soc.* **1999**, *121*, 4179–4188.
[12] L. C. Tabares, J. A. R. Navarro, J. M. Salas, *J. Am. Chem. Soc.* **2001**, *123*, 383–387.
[13] M. Albrecht, M. Lutz, A. L. Spek, G. van Koten, *Nature* **2000**, *406*, 970–974.
[14] K. Seki, *Phys. Chem. Chem. Phys.* **2002**, *4*, 1968–1972.
[15] D. Li, K. Kaneko, *Chem. Phys. Lett.* **2001**, *335*, 50–56.
[16] R. Kitaura, K. Fujimoto, S. Noro, M. Kondo, S. Kitagawa, *Angew. Chem.* **2002**, *114*, 141–143; *Angew. Chem. Int. Ed.* **2002**, *41*, 133–135.

Glycopeptide Synthesis

Toward Fully Synthetic *N*-Linked Glycoproteins**

*Justin S. Miller, Vadim Y. Dudkin, Gholson J. Lyon, Tom W. Muir, and Samuel J. Danishefsky**

The structural and biological consequences of cellular protein modification through posttranslational glycosylation are central issues in the rapidly growing field of glycobiology.[1] The availability of homogeneous glycopeptides, both *O*-linked (serine, threonine, or tyrosine α-glycosides) and *N*-linked (asparagine β-glycosides), could greatly enhance insight into glycobiology.[2] It became our view that the prospect of total synthesis of homogeneous glycoproteins provides the best chance for gaining such access.

Numerous methods exist for glycopeptide synthesis: glycans have been introduced into peptides by means of amino acid "cassettes" with pendant protected saccharides,[3] through enzymatic manipulations of glycopeptides,[4] or by conjugation of fully elaborated, complex saccharides to short synthetic peptides.[5] Larger *O*-linked glycopeptides have been synthesized by using ligation techniques[6] such as expressed protein ligation.[7] Bertozzi and co-workers extended the scope of the "cassette" approach by applying native chemical ligation to the synthesis of a biologically active glycoprotein with two single-residue *O*-linked glycans.[8] Tolbert and Wong described the ligation of a 392-residue intein-generated peptide thioester and a dipeptide functionalized with a single *N*-acetylglucosamine residue.[7c] Using a different fragment condensation protocol, Hojo et al. reported the synthesis of a glycopeptide domain of Emmprin that contains an *N*-linked chitobiose unit, but the saccharide was not entirely stable to the conditions required for resin cleavage in their solid-phase synthesis.[9]

[*] Prof. S. J. Danishefsky, Dr. J. S. Miller, Dr. V. Y. Dudkin
Laboratory for Bioorganic Chemistry
Sloan-Kettering Institute for Cancer Research
1275 York Avenue, New York, NY 10021 (USA)
Fax: (+1) 212-772-8691
E-mail: s-danishefsky@ski.mskcc.org
Prof. S. J. Danishefsky
Department of Chemistry, Columbia University
Havemeyer Hall, New York, NY 10027 (USA)
G. J. Lyon, Prof. T. W. Muir
Laboratory of Synthetic Protein Chemistry
The Rockefeller University
1230 York Avenue, New York, NY 10021 (USA)

[**] This work was supported by the NIH (AI16943). The receipt of a Pfizer Award to S.J.D. for Creative Work in Organic Synthesis is gratefully acknowledged. We thank Drs. Andrzej Zatorski and Ulrich Iserloh for the preparation of starting materials and for helpful discussions, and Dr. George Sukenick and Ms. Sylvi Rusli (NMR Core Facility, CA-02848) for mass spectral analyses.

Supporting information for this article is available on the WWW under http://www.angewandte.org or from the author. Experimental details include the preparation of and mass spectral characteristics for **2**–**6, 8**, and **10**–**12**; and NMR spectra for **5, 6, 8**, and **10**.